

Satellites capture soil moisture dynamics deeper than a few centimeters and are relevant to plant water uptake

Feldman Andrew¹, Gianotti Daniel², Dong Jianzhi², Akbar Ruzbeh², Crow Wade³, McColl Kaighin⁴, Nippert Jesse⁵, Tumber-Dávila Shersingh Joseph⁶, Holbrook Noel Michele⁴, Rockwell Fulton⁴, Scott Russell³, Reichle Rolf¹, Chatterjee Abhishek⁷, Joiner Joanna¹, Poulter Benjamin¹, and Entekhabi Dara²

¹NASA Goddard Space Flight Center

²Massachusetts Institute of Technology

³USDA ARS

⁴Harvard University

⁵Kansas State University

⁶Harvard Forest, Harvard University

⁷Jet Propulsion Laboratory

November 16, 2022

Abstract

A common viewpoint across the Earth science community is that global soil moisture estimates from satellite L-band (1.4 GHz) measurements represent moisture only in the shallow soil layers (0-5 cm) and are of limited value for studying global terrestrial ecosystems because plants use water from deeper rootzones. Here, we argue that such a viewpoint is flawed for two reasons. First, microwave soil emission theory and statistical considerations of vertically correlated soil moisture information together indicate that L-band measurements are typically representative of soil moisture within at least the top 15-25 cm, or 3-5 times deeper than commonly thought. Second, in reviewing isotopic tracer field studies of plant water uptake, we find a global prevalence of vegetation that primarily draws moisture from these upper soil layers. This is especially true for grasslands and croplands covering more than a third of global vegetated surfaces. While shrub and tree species tend to draw deeper soil moisture, these plants often still preferentially or seasonally draw water from the upper soil layers. Therefore, L-band satellite soil moisture estimates are more relevant to global vegetation water uptake than commonly appreciated, and we encourage their application across terrestrial hydrosphere and biosphere studies.

1 Satellites capture soil moisture dynamics deeper than a few centimeters and are
2 relevant to plant water uptake

3

4 Andrew F. Feldman^{1,2}, Daniel J. Short Gianotti³, Jianzhi Dong³, Ruzbeh Akbar³, Wade
5 T. Crow⁴, Kaighin A. McColl^{5,6}, Jesse B. Nippert⁷, Shersingh Joseph Tumber-Dávila⁸,
6 Noel M. Holbrook⁹, Fulton E. Rockwell⁹, Russell L. Scott¹⁰, Rolf H. Reichle¹¹, Abhishek
7 Chatterjee¹², Joanna Joiner¹³, Benjamin Poulter¹, Dara Entekhabi³

8

9 ¹Biospheric Sciences Laboratory, NASA Goddard Space Flight Center, Greenbelt, MD,
10 USA

11 ²NASA Postdoctoral Program, NASA Goddard Space Flight Center, Greenbelt, MD,
12 USA

13 ³Department of Civil and Environmental Engineering, Massachusetts Institute of
14 Technology, Cambridge, Massachusetts, USA

15 ⁴USDA ARS Hydrology and Remote Sensing Laboratory, Beltsville, Maryland, USA

16 ⁵Department of Earth and Planetary Sciences, Harvard University, Cambridge, MA, USA

17 ⁶Harvard John A. Paulson School of Engineering and Applied Sciences, Harvard
18 University, Cambridge, MA, USA

19 ⁷Division of Biology, Kansas State University, Manhattan, KS, USA

20 ⁸Harvard Forest, Harvard University, Petersham, MA, USA

21 ⁹Department of Organismic and Evolutionary Biology, Harvard University, Cambridge,
22 MA, USA

23 ¹⁰USDA ARS Southwest Watershed Research Center, Tucson, AZ, USA

24 ¹¹Global Modeling and Assimilation Office, NASA Goddard Space Flight Center,
25 Greenbelt, MD, USA

26 ¹²Jet Propulsion Laboratory, California Institute of Technology, Pasadena, CA, USA

27 ¹³Atmospheric Chemistry and Dynamics Laboratory, NASA Goddard Space Flight
28 Center, Greenbelt, MD, USA

29

30 **Abstract**

31 A common viewpoint across the Earth science community is that global soil moisture
32 estimates from satellite L-band (1.4 GHz) measurements represent moisture only in the
33 shallow soil layers (0-5 cm) and are of limited value for studying global terrestrial
34 ecosystems because plants use water from deeper rootzones. Here, we argue that such
35 a viewpoint is flawed for two reasons. First, microwave soil emission theory and
36 statistical considerations of vertically correlated soil moisture information together
37 indicate that L-band measurements are typically representative of soil moisture within at
38 least the top 15-25 cm, or 3-5 times deeper than commonly thought. Second, in
39 reviewing isotopic tracer field studies of plant water uptake, we find a global prevalence
40 of vegetation that primarily draws moisture from these upper soil layers. This is
41 especially true for grasslands and croplands covering more than a third of global
42 vegetated surfaces. While shrub and tree species tend to draw deeper soil moisture,
43 these plants often still preferentially or seasonally draw water from the upper soil layers.
44 Therefore, L-band satellite soil moisture estimates are more relevant to global

45 vegetation water uptake than commonly appreciated, and we encourage their
46 application across terrestrial hydrosphere and biosphere studies.

47

48 **1. Introduction**

49 Global soil moisture retrievals from microwave satellites are now widely used across the
50 Earth science community to study various topics related to the global climate system
51 and its water, carbon, and energy cycles. While soil moisture in the unsaturated zone
52 stores only 0.005% of Earth's water by volume (Bras, 1990), its position at the interface
53 of the land and the atmosphere is of high value for understanding these global cycles
54 (Koster and Suarez, 2001; McColl et al., 2017). As such, satellite-based soil moisture
55 estimates are increasingly being used in studies of land-atmosphere interactions,
56 numerical weather prediction, plant function and stress, and land surface response to
57 climate change (Akbar et al., 2020; Dong et al., 2020; Feldman et al., 2018b, 2022;
58 Konings et al., 2017; Purdy et al., 2018; Santanello et al., 2019; Short Gianotti et al.,
59 2020; Taylor et al., 2012; Tuttle and Salvucci, 2016).

60

61 However, a viewpoint has spread that microwave satellite soil moisture is of limited use
62 for studying vegetated landscapes because it only perceives the surface layer of deep
63 rootzones. A major contributor to this viewpoint is the history of the microwave remote
64 sensing community generally offering a simplified view of a shallow observing depth of
65 satellite-based retrievals. For example, the Soil Moisture Active Passive (SMAP) and
66 Soil Moisture and Ocean Salinity (SMOS) L-band satellite missions are often described
67 as producing estimates of soil moisture within the top 5 cm of soil (Entekhabi et al.,
68 2010; Kerr et al., 2010). Similarly, the Advanced Microwave Scanning Radiometer
69 (AMSR) satellite series and the Advanced Scatterometer (ASCAT) (at higher C- and X-
70 band frequencies) are thought to observe only the top 2 cm of soil. Other contributors to
71 this viewpoint include the prevalent use of the top-most in-situ sensors for assessing
72 satellite soil moisture products, and a common intuition that the maximum rooting depth
73 defines the relevant water uptake profile.

74

75 According to this viewpoint, if roots supply plants from soil layers down to maximum
76 rooting depths that are meters below the top 5 cm, then satellite soil moisture estimates
77 have little value for the global study of terrestrial water, carbon, and energy fluxes, given
78 that these fluxes can rely heavily on plant use of soil moisture (Jasechko et al., 2013;
79 Katul et al., 2012). As a result, many researchers avoid the use of these microwave
80 satellite soil moisture products, instead often favoring rootzone moisture products from
81 model reanalysis or precipitation-based wetness indices. We avoid calling attention to
82 specific references, but argue that such a viewpoint is widely held and is stated across
83 the peer-reviewed literature. If satellite soil moisture retrievals were to hold more
84 information about the rootzone, they would be considered more desirable than
85 reanalysis products for some land-atmosphere and ecological applications; they are
86 observations independent of model-prescribed linkages with other land surface
87 variables and provide direct information about plant water use and evapotranspiration
88 (Dong and Crow, 2019).

89

90 In fact, recent studies do not support the idea that microwave satellites are limited to
91 seeing only a shallow (0-5 cm) surface soil layer. The same L-band microwaves used to
92 retrieve surface soil moisture have been previously used to detect subsurface geologic
93 features in drylands beyond depths of one meter (Farr et al., 1986; Paillou et al., 2010).
94 Even if soil moisture satellites only observed the upper soil layers, surface and rootzone
95 moisture dynamics are almost always hydraulically connected and correlated (Akbar et
96 al., 2018; Ford et al., 2014; Qiu et al., 2014). This is because rootzone moisture is
97 driven by surface forcing and has strong spatiotemporal memory resulting in similar soil
98 moisture dynamics in the upper surface and deeper soil layers (Albergel et al., 2008;
99 McColl et al., 2017). Hydraulic redistribution by plants can also further couple the
100 surface and deeper soil layers (Nadezhdina et al., 2010). As a result, the vertical depth
101 of representation, or support scale, of L-band satellite surface soil moisture has been
102 shown to be deeper than 5 cm (Akbar et al., 2018; Short Gianotti et al., 2019). Both
103 surface and deeper soil layer support scales consequently have similar information
104 content in explaining evapotranspiration fluxes and moisture thresholds between
105 evaporative regimes (Dong et al., 2022; Qiu et al., 2016). Satellite surface soil moisture
106 retrievals are thus recognized as a means to improve the characterization of rootzone
107 soil moisture and evapotranspiration in model assimilation frameworks (Kumar et al.,
108 2009; Purdy et al., 2018; Reichle et al., 2019).

109
110 Furthermore, a common emphasis on the fact that maximum rooting depths can extend
111 plant water uptake meters into the soil (Nepstad et al., 1994) neglects that active water
112 uptake is rarely uniform across the rooting profile. Specifically, global observations and
113 optimally modeled rooting profiles indicate that most plants preferentially draw water
114 from the upper soil layers to take advantage of these layers' pulse water and nutrient
115 availability (Collins and Bras, 2007; Jackson et al., 1996; Nippert and Holdo, 2015).
116 Even for deeper-rooted vegetation, high sensitivity to upper-layer soil moisture is also
117 found based on findings of decreasing rooting biomass and root hydraulic conductance
118 with depth (Nippert et al., 2012; Werner et al., 2021). Therefore, to learn about nominal
119 plant water use and evapotranspiration, rootzone soil moisture products may not always
120 need to integrate moisture dynamics down to the maximum rooting depth.

121
122 This perspective article evaluates the literature to determine (1) whether L-band satellite
123 surface soil moisture products capture soil moisture dynamics deeper than 5 cm and (2)
124 to what extent the vertical soil depth representation of satellite retrievals is relevant for
125 global vegetation water uptake and evapotranspiration.

126 127 **2. Satellite Soil Moisture's Effective Sensing Depth**

128 The true vertical support of remote sensing-based soil moisture retrievals is dependent
129 on both (1) the microwave emission properties of the soil column and (2) the vertical
130 autocorrelation of typical soil moisture profiles and their dynamics (Njoku and
131 Entekhabi, 1996; Short Gianotti et al., 2019). Both principles result in decay of soil
132 moisture representation with depth (i.e., exponential distribution). Furthermore, these
133 principles trade off in dominance from dry to wet conditions (Fig. 1).

134

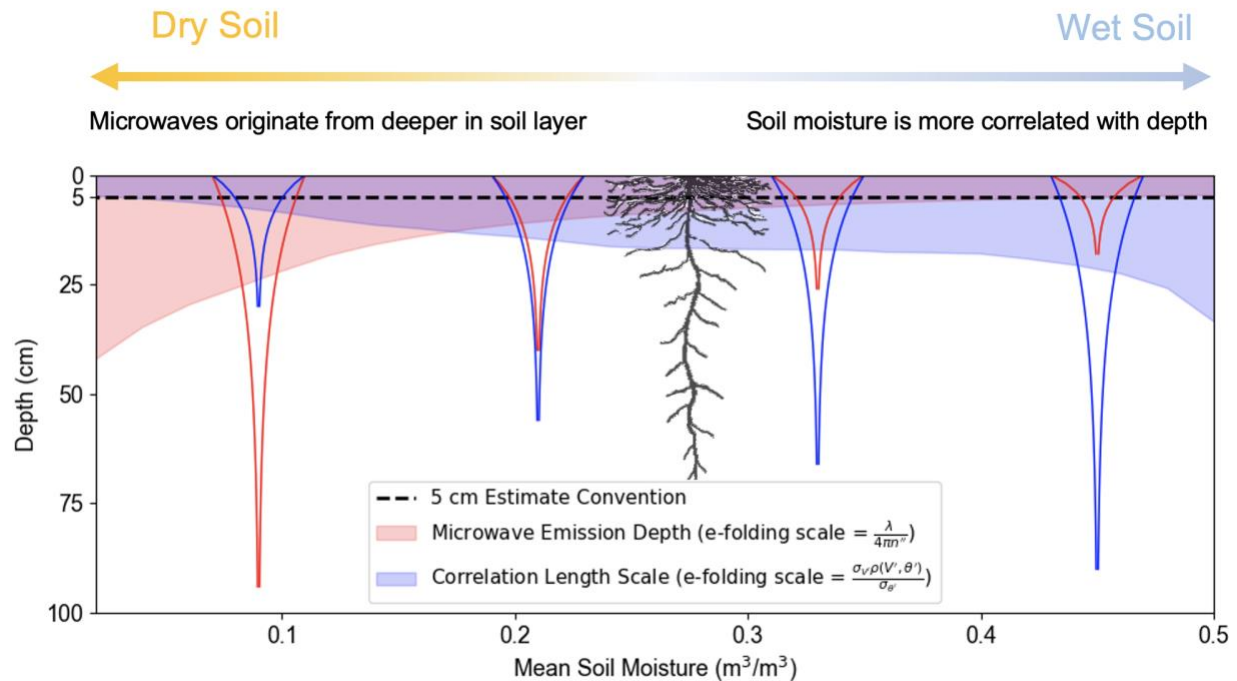
135 For drier soils, L-band satellites directly detect soil moisture in a deeper soil column
136 because microwave emission originates from deeper soil layers (Fig. 1). Specifically,
137 modeling microwave emission from a soil layer that is assumed to be a homogenous,
138 dielectric medium reveals that soil emission depth increases with aridity and vertically
139 decays approximately exponentially (Njoku and Entekhabi, 1996; Njoku and Kong,
140 1977). Therefore, despite drier periods resulting in less coupling between surface and
141 deeper layer soil moisture, satellites directly sample deeper into the soil column, often
142 well below 5 cm (Fig. 1).

143
144 For wetter soils, despite shallower soil emission depths from an electromagnetic
145 perspective, surface soil moisture has a greater hydraulic connectivity with deeper soil
146 layers (Fig. 1). This is because soil moisture is a storage variable with strong
147 spatiotemporal memory (McColl et al., 2017). As a result, satellite soil moisture from L-
148 band satellites holds statistical information about the soil moisture magnitudes and
149 variations deeper than 5 cm into the soil column, especially under wetter conditions
150 (Akbar et al., 2018; Short Gianotti et al., 2019). Such vertical autocorrelation information
151 decays approximately exponentially with depth, similarly to microwave soil emission.

152
153 Combining these electromagnetic and statistical considerations shows that, under a
154 wide range of soil moisture conditions, L-band satellites effectively sample soil moisture
155 dynamics deeper than 5 cm - realistically the top 15 to 25 cm (Fig. 1). This deeper
156 “effective sensing depth” results from electromagnetic and statistical considerations of
157 satellite-based soil moisture trading off in their dominance of vertical soil representation
158 from dry to wet conditions. In principle, the combined support scale of the satellite-
159 based soil moisture dynamics is at least the deeper of the two considerations, the full
160 depth of which is under investigation. Deeper layers between 25 to 100 cm are still
161 integrated but contribute progressively less to the signal with depth (Fig. 1). By contrast,
162 reanalysis rootzone moisture products often assess the uniform, column-averaged soil
163 moisture typically between 0 and 100 cm and/or discretized portions of this range.

164
165 Note that, in the case of drier soils, the microwave emission depth directly observes the
166 magnitude and time variations of deeper layer soil moisture. However, in wetter
167 conditions, only the soil moisture magnitude and variations in the upper soil layers
168 nearer to 5 cm are directly observed by L-band satellite sensors (Fig. 1). Nevertheless,
169 the typically high hydraulic connectivity between shallow and deeper layers in these
170 wetter conditions allows indirect observation of the soil moisture magnitude and
171 variations in the deeper layers.

172



173
 174 Figure 1. Effective sensing depth of microwave satellite soil moisture based on
 175 consideration of both L-band (1.4 GHz) microwave soil emission physics and vertical
 176 hydraulic connectivity of soil moisture. Satellite effective sensing depths of soil moisture
 177 range between 15 cm to over 25 cm, 3-5 times deeper than commonly thought, while
 178 integrating some deeper soil information. Effective sensing depths (shading) are e-
 179 folding scales determined from distributions (solid lines) of microwave soil emission and
 180 soil moisture information with depth. Microwave emission depth e-folding scale (red
 181 shading) and example emission profiles (red solid lines) are computed based on the soil
 182 emission model in Njoku and Entekhabi, (1996). Note that changes in soil texture have
 183 minimal influence on microwave emission depths compared to variations in soil
 184 moisture (not shown). E-folding vertical correlation length scales (blue shading) are
 185 computed by averaging global vertical length scale estimates, obtained with permission
 186 from Short Gianotti et al., (2019), binned based on mean annual soil moisture.
 187 Corresponding example profiles of degree of hydraulic connectivity with the surface
 188 (blue solid lines) are estimated from these averaged e-folding length scales. For
 189 equation details, see Appendix A. The displayed root profile image, adapted with
 190 permission from Nippert and Holdo, (2015), has a commonly-observed structure of
 191 decreasing root biomass with depth. The exact dimensions vary globally.

192
 193 **3. Revised View of Plant Water Uptake Depths**

194 A common viewpoint across the Earth science community is that rootzones are
 195 (qualitatively) “deep,” which strongly argues against using a 0-5-cm or even a 0-20-cm
 196 soil moisture dataset to study vegetated landscapes. Indeed, maximum rooting depths
 197 often extend to 1-2-m and, at times, tens of meters below the surface depending on
 198 climate and surface topography (Fan et al., 2017; Nepstad et al., 1994; H. J. Schenk
 199 and Jackson, 2002; Tumber-Dávila et al., 2022). Existence of deep roots indicates
 200 adaptation to plant water stress, where access to deeper, less variable water sources

201 allows plants to continue transpiring and survive under severe water-limitation (Stocker
202 et al., 2021). However, in the context of nominal plant water uptake, such a perspective
203 can result in over-emphasis of the maximum rooting depth and neglect of the nature of
204 typical rooting profiles and their relevance to the global water cycle. Specifically, global
205 rooting profiles are typically concentrated in the upper soil layers and decrease in root
206 density with depth (Jackson et al., 1996). For example, some estimates indicate that
207 90% of global vegetation has more than half of their roots in the top 30 cm of soil (J. H.
208 Schenk and Jackson, 2002).

209
210 Shallow preferential soil water uptake and deeper roots can exist concurrently - the
211 existence of a deep maximum rooting depth does not imply low plant utilization of
212 shallow soil moisture. The deepest roots are indeed important for survival under
213 seasonal or severe water limitation. However, the frequency and volumetric proportion
214 of use of these deeper water stores is small, often much less than 10% of annual plant
215 water uptake (McCormick et al., 2021; Miguez-Macho and Fan, 2021). This lower
216 contribution of water uptake from the deeper layers is, in part, because there are
217 hydraulic limitations in transporting water over long vertical distances from deeper roots,
218 with high radial and axial resistances in roots that can increase with depth (Jones, 2014;
219 Landsberg and Fowkes, 1978; Nippert et al., 2012). Additionally, essential limiting
220 nutrients are typically highly concentrated in the upper soil layers due to decaying
221 organic matter, which prevents sole plant reliance on deeper moisture sources
222 (Jobbágy and Jackson, 2001). This motivates strategies like hydraulic redistribution
223 where plants actively move water via the roots to upper soil layers for easier uptake of
224 nutrients under dry conditions (Cardon et al., 2013). As such, the maximum rooting
225 depth is often of limited importance for evaluating nominal plant water uptake
226 throughout the year (Nippert and Holdo, 2015). This is true even in water-limited
227 ecosystems (Nippert and Holdo, 2015), where rainfall infiltration is often shallow (<30
228 cm) and plants must rely on this more frequently wetted shallow zone for survival (Scott
229 and Biederman, 2019).

230
231 Additionally, due to root suberization and woody root development that prevents root
232 water uptake, the rooting distribution does not necessarily match the actual vertical
233 profile of root water uptake (Kramer and Boyer, 1995). Instead, isotopic tracers can be
234 used to estimate the true range of primary water uptake, commonly called the functional
235 rooting profile (Dawson and Pate, 1996; Ehleringer and Dawson, 1992). Within the limits
236 imposed by isotopic mixing model uncertainties (Case et al., 2020; Ogle et al., 2004),
237 isotopic tracer methods can determine water uptake profiles and/or ranges more
238 relevant to the water cycle than knowledge of the rooting profile alone.

239
240 Therefore, instead of rooting profile information, we have collated isotopic tracer studies
241 that determine the vertical range of roots contributing the most to xylem water within
242 plants (Fig. 2). Values displayed in Fig. 2 reflect the primary zones of water uptake over
243 most of the year indicated by each reviewed study. In our web search of peer-reviewed
244 literature, our keywords included “stable”, “isotope”, “tracer”, “plant”, “root”, “water
245 uptake,” and “soil.” We only sampled studies that (a) explicitly stated or displayed the
246 primary depths of water uptake (avoiding subjective judgment of results), (b) assessed

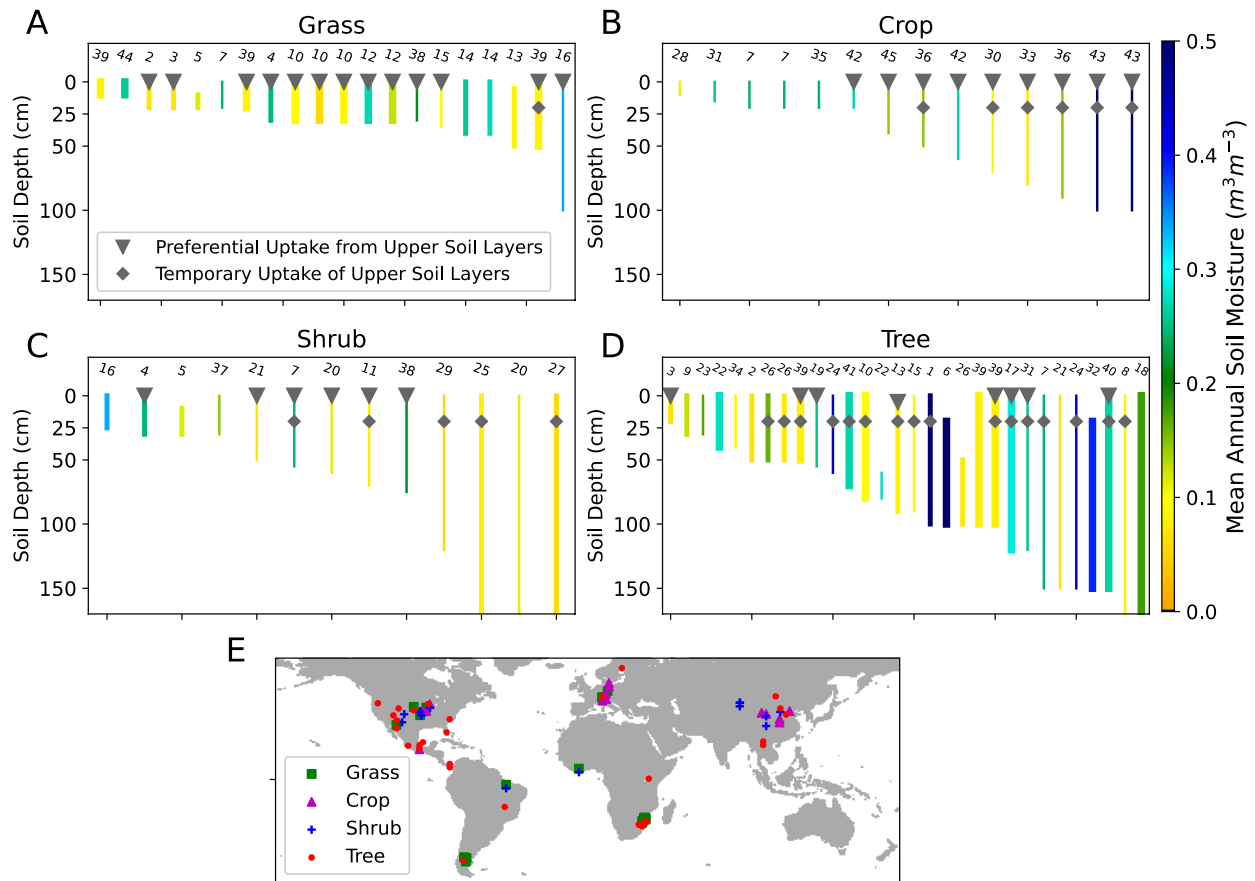
247 naturally occurring plants under nominal conditions (avoiding experimental
248 manipulation, extreme stress, and laboratory experiments), and (c) evaluated plant
249 species with an unobstructed rootzone (avoiding riparian, coastal, and shallow bedrock
250 environments). We additionally searched citations within studies that initially met our
251 criteria using these same keywords. Our search resulted in 45 references that met our
252 criteria (Fig. 2 and Table S1).

253
254 We find that grass and crop species across global climates typically extract water from
255 the upper soil layers (0-30 cm) over most of the year, with preferential uptake of water
256 nearer to the surface (Figs. 2A and 2B). For grass species, 95% of the studies found
257 grasses primarily use water from at least the top 50 cm with 65% of studies explicitly
258 finding increased proportional uptake in the top-most soil layers (Fig. 2A). All sampled
259 crop species either primarily use soil water within the top 25 cm or preferentially draw
260 water from the upper soil layers with decreasing water use with depth (Fig. 2B). All crop
261 studies that found water use extending deeper than 50 cm also found proportionally
262 higher water use in the upper soil layers. 88% of these same studies also found the
263 primary plant water uptake zone transitioned temporarily to the upper soil layers (see
264 diamond symbols in Fig. 2B).

265
266 Shrub and tree species show a larger vertical range of water uptake, with water uptake
267 commonly extending to well below 50 cm (Figs. 2C and 2D) often related to root-niche
268 separation under competition with grasses (Case et al., 2020). However, even in these
269 deeper water uptake cases, 89% of shrub isotopic studies and 67% of tree isotopic
270 studies found either proportionally higher water uptake from the upper soil layers or the
271 primary water use zone transitioned temporarily to the upper soil layers. Absence of
272 triangle and diamond symbols indicate that the study did not mention either
273 phenomenon, not that the phenomenon does not exist. Therefore, these percentages
274 that indicate preferential or temporary uptake of upper soil layer moisture are lower
275 bounds.

276
277 We acknowledge potential biases in our search. For example, a greater proportion of
278 studies in the midlatitudes arises due to abundant field research facilities in Asia,
279 Europe, and North America as well as a lack of field measurements in the tropics
280 (Schimel et al., 2015). More studies also take place in semi-arid and sub-humid
281 environments because of their higher proportion of global land cover (about 70% of land
282 surfaces receive <1,000 mm of annual rainfall according to Global Precipitation
283 Measurement rainfall (Huffman, 2015)). While our search yielded few tropical forest
284 studies, we expect these regions may have deeper functional rooting profiles similarly to
285 those found in Fig. 2D (Ichii et al., 2007). However, we argue that this search provided a
286 representative distribution of species across grass, crop, shrub, and tree categories and
287 across global moisture availability gradients.

288



289
 290 Figure 2. Primary root water uptake profiles (or functional rooting profile) based on field
 291 stable isotope tracer studies for species binned in (A) grass, (B) crop, (C) shrub, and (D)
 292 tree categories based on Table S1. The triangle symbol means the study found
 293 preferential water uptake nearer to the surface and decreasing uptake with depth. The
 294 diamond symbol means that while the study found uptake to 50 cm soil depths or below,
 295 root water uptake switched primarily to the upper soil layers (~ 30 cm) temporarily
 296 during the year. Placement of the diamond symbol at 20 cm is arbitrary. Thickness of
 297 the line indicates number of species studied in the given reference. The number above
 298 the plotlines is the reference index (see Table S1). Mean annual SMAP soil moisture is
 299 displayed for each field site using the nearest 36 km pixel. (E) Locations of the isotopic
 300 field measurements.

301
 302 **4. Recommendations**

303 Our findings convey that satellite L-band radiometry captures global soil moisture
 304 dynamics at least as deep as the top 15-25 cm of soil (Fig. 1), which is more than three
 305 times deeper than commonly stated as well as more relevant for evaluating plant
 306 function than commonly appreciated. L-band satellite soil moisture estimates appear
 307 optimal for studying most grasslands and croplands, which cover more than a third of
 308 global vegetated surfaces. This proportion is higher when including non-vegetated
 309 surfaces, given that bare surfaces are also dominated by upper soil layer processes
 310 (i.e., bare soil evaporation). Grass and crop water use also decreases with depth, much

311 like the decreasing L-band satellite soil moisture representation with depth (Fig. 1).
312 Therefore, soil moisture datasets that integrate rootzone dynamics between 0-100 cm
313 and deeper may in fact be less useful than L-band soil moisture for representing plant-
314 relevant soil moisture dynamics in grass and croplands. This is because soil moisture
315 products representing the 0-100 cm layer will integrate subdued moisture dynamics in
316 deeper layers not relevant to the functional rooting profile concentrated in the upper soil
317 layers. Additionally, even woody plant species that exhibit deeper root water uptake
318 (shrubs and trees; see Fig. 2) frequently draw water nearer to the surface preferentially
319 or temporarily within a given season. L-band soil moisture observations are still useful
320 for these scenarios at least during certain times of the year, and will increase in utility if
321 global functional root profiles become shallower under global change (Hauser et al.,
322 2020).

323
324 Given these considerations, our findings indicate a wider applicability of satellite soil
325 moisture for the study of global climate. This encourages broader, more confident use of
326 satellite soil moisture for the study of soil moisture's impact on the terrestrial net carbon
327 balance, water movement in the soil-plant-atmosphere continuum, land-atmosphere
328 coupling, and crop yield forecasting (Akbar et al., 2020; Dong et al., 2020; Feldman et
329 al., 2022, 2018b; Konings et al., 2017; Purdy et al., 2018; Santanello et al., 2019; Short
330 Gianotti et al., 2020; Taylor et al., 2012; Tuttle and Salvucci, 2016).

331
332 While our assessment indicates wide applicability of L-band satellite soil moisture, we
333 stress that deeper-layer (0-100 cm and beyond) soil moisture products based on the
334 assimilation of L-band observations (i.e., SMAP L4 rootzone soil moisture; Reichle et
335 al., 2019) are likely more optimal for the study of soil moisture memory in the context of
336 land-atmosphere interactions, the study of deeper-rooted vegetation function under
337 water-stress conditions, the study of infiltration and drainage fluxes, and the initialization
338 of dynamical seasonal forecasts. Our findings here also indicate that reanalysis
339 rootzone soil moisture products are needed for the study of many mixed (i.e., savanna)
340 and forested landscapes.

341
342 Furthermore, we argue that there is no single soil moisture product that will globally
343 integrate the soil moisture layers relevant to plant water uptake and thus terrestrial
344 water, carbon, and energy exchanges. Instead, the optimal soil moisture product
345 changes in time and space. For studies of water, carbon, and energy exchanges at
346 landscape scales, we encourage first understanding the typical root water uptake
347 patterns for plant species in the study region and then carefully selecting a soil moisture
348 dataset. Potentially, multiple products and their synergistic use are needed depending
349 on the complexity of root water uptake scenarios.

350
351 For example, for herbaceous ecosystems including most croplands, grasslands, and
352 savannas with sparse tree cover, the L-band soil moisture products will likely optimally
353 integrate the relevant rootzone moisture information. These observations will
354 additionally be optimal for the study of mostly bare surface supplied mainly by soil
355 evaporation. Alternatively, in scenarios where prevalent deeper-rooted shrubs and trees
356 are mixed with a shallow-rooted understory, datasets representing a uniform distribution

357 of integrated soil moisture across the top 1-2 meters of soil (i.e., model reanalysis
 358 rootzone soil moisture products) may be optimal (Reichle et al., 2019). P-band (0.4
 359 GHz) soil moisture remote sensing applications may be more useful for these scenarios
 360 as well with potentially twice as deep of effective sensing depths than at L-band
 361 (Konings et al., 2014). Finally, in scenarios where root water uptake extends well below
 362 one meter for consistent or transient use of deep moisture or groundwater (McCormick
 363 et al., 2021; Miguez-Macho and Fan, 2021), care must be taken in determining when
 364 this uptake occurs. Such scenarios may occur in tropical rainforests where L-band
 365 satellite soil moisture retrievals are suboptimal due to vegetation multiple-scattering of
 366 microwaves (Feldman et al., 2018a; Kurum et al., 2011). Satellite-based terrestrial water
 367 storage variations (i.e., GRACE and GRACE-FO) may be useful to study these cases
 368 and can be used in tandem with reanalysis rootzone products (Rodell and Famiglietti,
 369 2001).

370
 371 In summary, we urge the community to consider using L-band soil moisture
 372 observations for applications involving vegetated landscapes. The value of satellite-
 373 based soil moisture beyond only a shallow (0-5 cm) surface layer emphasizes the
 374 urgent need to maintain continuity of L-band satellite remote sensing missions.

375 **Appendix A**

376 The e-folding depth of microwave emission used to estimate surface soil moisture can
 377 be modeled by:

$$378 L_{Emission} = \frac{\lambda}{4\pi n''} \quad (\text{Eq. A1})$$

379 where λ is the emission wavelength (Njoku and Kong, 1977). n'' is the imaginary part of
 380 the refractive index, which is the square root of the dielectric constant. The dielectric
 381 constant is a function largely of soil moisture and soil texture (i.e., clay fraction). $L_{Emission}$
 382 is the e-folding scale that represents the emission depth of microwaves. Measurements
 383 of these microwaves are used to estimate satellite soil moisture.

384
 385
 386 The e-folding vertical correlation length scale of soil moisture dynamics can be
 387 computed by:

$$388 L_{Correlation} = \frac{\sigma_{V'} \rho(V', \theta_s')}{\sigma_{\theta_s'}} \quad (\text{Eq. A2})$$

389 where V is the total volume soil moisture in the column, θ_s is the surface soil moisture, ρ
 390 is correlation, and σ is standard deviation (Short Gianotti et al., 2019). Prime
 391 superscripts indicate the time derivative. $L_{Correlation}$ is a correlation length scale, or the e-
 392 folding scale, that captures the decay of surface soil moisture's correlation with the total
 393 column soil moisture. $L_{Correlation}$ is thus the effective depth to which the surface soil
 394 moisture (here, being measured at least at a 5 cm depth) holds information about the
 395 total soil column moisture. Similar theoretical arguments allow interpretation of $L_{Correlation}$
 396 to be a support scale of the soil moisture magnitude and time dynamics (Akbar et al.,
 397 2018).

398
 399 While Eq. A2 is an exact solution, total column volumetric moisture is not widely
 400 available to estimate $L_{Correlation}$ globally. Thus, Short Gianotti et al. (2019) estimate
 401 $L_{Correlation}$ using information about the variance of surface hydrologic fluxes (rainfall

402 minus surface hydrologic losses) as well as surface soil moisture variance and
403 autocorrelation (their equation 28). GPM rainfall retrievals and SMAP soil moisture
404 retrievals are used together to globally estimate $L_{\text{Correlation}}$, which are used in Fig. 1.

405

406 **Acknowledgements**

407 Andrew F. Feldman's research was supported by an appointment to the NASA
408 Postdoctoral Program at the NASA Goddard Space Flight Center, administered by Oak
409 Ridge Associated Universities under contract with NASA. The authors with MIT
410 affiliation, Rolf H. Reichle, and Wade T. Crow were supported by the NASA SMAP
411 mission. The authors thank Alexandra Konings for helpful comments that improved the
412 manuscript.

413

414 **Author Contributions**

415 A.F.F. conceived of the study, performed the analysis, and drafted the manuscript. D.E.
416 and A.F.F. led the study. D.J.S.G., J.D., R.A., W.T.C, and D.E. provided guidance and
417 edits on the presentation of satellite sensing depth estimates. J.B.N., S.J.T.D, N.M.H.,
418 F.E.R., and R.L.S. provided guidance and edits on presentation of isotopic tracer
419 studies and rooting depth information. K.A.M., R.H.R., A.C., J.J., and B.P. provided
420 guidance on all components and, in particular, in framing the perspective in the context
421 of their respective fields. All authors contributed substantial textual edits.

422

423 **References**

- 424 Akbar, R., Short Gianotti, D., McColl, K.A., Haghghi, E., Salvucci, G.D., Entekhabi, D.,
425 2018. Hydrological Storage Length Scales Represented by Remote Sensing
426 Estimates of Soil Moisture and Precipitation. *Water Resour. Res.* 1476–1492.
427 <https://doi.org/10.1002/2017WR021508>
- 428 Akbar, R., Short Gianotti, D.J., Salvucci, G.D., Entekhabi, D., 2020. Partitioning of
429 Historical Precipitation Into Evaporation and Runoff Based on Hydrologic Dynamics
430 Identified With Recent SMAP Satellite Measurements. *Water Resour. Res.* 56, 1–
431 21. <https://doi.org/10.1029/2020WR027307>
- 432 Albergel, C., Rüdiger, C., Pellarin, T., Calvet, J.C., Fritz, N., Froissard, F., Suquia, D.,
433 Petitpa, A., Pignatelli, B., Martin, E., 2008. From near-surface to root-zone soil
434 moisture using an exponential filter: An assessment of the method based on in-situ
435 observations and model simulations. *Hydrol. Earth Syst. Sci.* 12, 1323–1337.
436 <https://doi.org/10.5194/hess-12-1323-2008>
- 437 Bras, R.L., 1990. *Hydrology: An Introduction to Hydrologic Science*. Addison-Wesley
438 Publishing Co., Inc.
- 439 Cardon, Z.G., Stark, J.M., Herron, P.M., Rasmussen, J.A., 2013. Sagebrush carrying
440 out hydraulic lift enhances surface soil nitrogen cycling and nitrogen uptake into
441 inflorescences. *Proc. Natl. Acad. Sci. U. S. A.* 110, 18988–18993.
442 <https://doi.org/10.1073/pnas.1311314110>
- 443 Case, M.F., Nippert, J.B., Holdo, R.M., Staver, A.C., 2020. Root-niche separation
444 between savanna trees and grasses is greater on sandier soils. *J. Ecol.* 108, 2298–
445 2308. <https://doi.org/10.1111/1365-2745.13475>
- 446 Collins, D.B.G., Bras, R.L., 2007. Plant rooting strategies in water-limited ecosystems.
447 *Water Resour. Res.* 43, 1–10. <https://doi.org/10.1029/2006WR005541>

448 Dawson, T.E., Pate, J.S., 1996. Seasonal water uptake and movement in root systems
449 of Australian phraeatophytic plants of dimorphic root morphology: A stable isotope
450 investigation. *Oecologia* 107, 13–20. <https://doi.org/10.1007/BF00582230>

451 Dong, J., Akbar, R., Gianotti, D.J.S., Feldman, A.F., Crow, W.T., Entekhabi, D., 2022.
452 Can Surface Soil Moisture Information Identify Evapotranspiration Regime
453 Transitions? *Geophys. Res. Lett.* e2021GL097697.

454 Dong, J., Crow, W.T., 2019. L-band remote-sensing increases sampled levels of global
455 soil moisture-air temperature coupling strength. *Remote Sens. Environ.* 220, 51–
456 58. <https://doi.org/10.1016/j.rse.2018.10.024>

457 Dong, J., Dirmeyer, P.A., Lei, F., Anderson, M.C., Holmes, T.R.H., Hain, C., Crow,
458 W.T., 2020. Soil Evaporation Stress Determines Soil Moisture-Evapotranspiration
459 Coupling Strength in Land Surface Modeling. *Geophys. Res. Lett.* 47, 1–11.
460 <https://doi.org/10.1029/2020GL090391>

461 Ehleringer, J.R., Dawson, T.E., 1992. Water uptake by plants: perspectives from stable
462 isotope composition. *Plant, Cell Environ.* [https://doi.org/10.1111/j.1365-](https://doi.org/10.1111/j.1365-3040.1992.tb01657.x)
463 3040.1992.tb01657.x

464 Entekhabi, D., Njoku, E.G., O'Neill, P.E., Kellogg, K.H., Crow, W.T., Edelstein, W.N.,
465 Entin, J.K., Goodman, S.D., Jackson, T.J., Johnson, J., Kimball, J., Piepmeier, J.R.,
466 Koster, R.D., Martin, N., McDonald, K.C., Moghaddam, M., Moran, S., Reichle, R.,
467 Shi, J.C., Spencer, M.W., Thurman, S.W., Tsang, L., Van Zyl, J., 2010. The Soil
468 Moisture Active Passive (SMAP) Mission. *Proc. IEEE* 98, 704–716.
469 <https://doi.org/10.1109/JPROC.2010.2043918>

470 Fan, Y., Miguez-Macho, G., Jobbágy, E.G., Jackson, R.B., Otero-Casal, C., 2017.
471 Hydrologic regulation of plant rooting depth. *Proc. Natl. Acad. Sci. U. S. A.* 114,
472 10572–10577. <https://doi.org/10.1073/pnas.1712381114>

473 Farr, T.G., Elachi, C., Hartl, P., Chowdhury, K., 1986. Microwave Penetration and
474 Attenuation in Desert Soil: A Field Experiment with the Shuttle Imaging Radar.
475 *IEEE Trans. Geosci. Remote Sens.* GE-24, 590–594.
476 <https://doi.org/10.1109/TGRS.1986.289675>

477 Feldman, A.F., Akbar, R., Entekhabi, D., 2018a. Characterization of Higher-Order
478 Scattering from Vegetation with SMAP Measurements. *Remote Sens. Environ.* 219,
479 324–338.

480 Feldman, A.F., Entekhabi, D., Gianotti, D.J.S., Trigo, I.F., Salvucci, G.D., 2022.
481 Observed Landscape Responsiveness to Climate Forcing. *Water Resour. Res.* 58,
482 e2021WR030316.

483 Feldman, A.F., Short Gianotti, D.J., Konings, A.G., McColl, K.A., Akbar, R., Salvucci,
484 G.D., Entekhabi, D., 2018b. Moisture pulse-reserve in the soil-plant continuum
485 observed across biomes. *Nat. Plants* 4, 1026–1033.
486 <https://doi.org/10.1038/s41477-018-0304-9>

487 Ford, T.W., Harris, E., Quiring, S.M., 2014. Estimating root zone soil moisture using
488 near-surface observations from SMOS. *Hydrol. Earth Syst. Sci.* 18, 139–154.
489 <https://doi.org/10.5194/hess-18-139-2014>

490 Hauser, E., Sullivan, P.L., Flores, A., Billings, S.A., 2020. Global-scale shifts in
491 Anthropocene rooting depths pose unexamined consequences in critical zone
492 functioning. *Earth Sp. Sci. Open Arch.*

493 Huffman, G., 2015. GPM Level 3 IMERG Final Run Half Hourly 0.1 × 0.1 Degree

494 Precipitation, version 05 (Goddard Space Flight Center Distributed Active Archive
495 Center (GSFC DAAC), 2015).

496 Ichii, K., Hashimoto, H., White, M.A., Potter, C., Hutyyra, L.R., Huete, A.R., Myneni, R.B.,
497 Nemani, R.R., 2007. Constraining rooting depths in tropical rainforests using
498 satellite data and ecosystem modeling for accurate simulation of gross primary
499 production seasonality. *Glob. Chang. Biol.* 13, 67–77.
500 <https://doi.org/10.1111/j.1365-2486.2006.01277.x>

501 Jackson, R.B., Canadell, J., Ehleringer, J.R., Mooney, H.A., Sala, O.E., Schulze, E.D.,
502 1996. A global analysis of root distributions for terrestrial biomes. *Oecologia* 108,
503 389–411. <https://doi.org/10.1007/BF00333714>

504 Jasechko, S., Sharp, Z.D., Gibson, J.J., Birks, S.J., Yi, Y., Fawcett, P.J., 2013.
505 Terrestrial water fluxes dominated by transpiration. *Nature* 496, 347–350.
506 <https://doi.org/10.1038/nature11983>

507 Jobbágy, E.G., Jackson, R.B., 2001. The distribution of soil nutrients with depth: Global
508 patterns and the imprint of plants. *Biogeochemistry* 53, 51–77.
509 <https://doi.org/10.1023/A:1010760720215>

510 Jones, H.G., 2014. *Plants and Microclimate: A Quantitative Approach to Environmental*
511 *Plant Physiology*, 3rd ed. Cambridge University Press, Cambridge, UK.

512 Katul, G.G., Oren, R., Manzoni, S., Higgins, C., Parlange, M.B., 2012.
513 Evapotranspiration: A process driving mass transport and energy exchange in the
514 soil-plant-atmosphere-climate system. *Rev. Geophys.* 50.
515 <https://doi.org/10.1029/2011RG000366>

516 Kerr, Y., Waldteufel, P., Wigneron, J.-P., Delwart, S., Cabot, F., Boutin, J., Escorihuela,
517 M.J., Font, J., Reul, N., Gruhier, C., Juglea, S.E., Drinkwater, M.R., Achim HReul,
518 N., Boutin, J., Gruhier, C., Juglea, S.E., Drinkwater, M.R., Hahne, A., Neira, M.M.-,
519 Mecklenburg, S., 2010. The SMOS Mission: New Tool for Monitoring Key Elements
520 of the Global Water Cycle. *Proc. IEEE* 98, 666–687.

521 Konings, A.G., Entekhabi, D., Moghaddam, M., Saatchi, S.S., 2014. The Effect of a
522 Variable Soil Moisture Profile on P-band Backscatter Estimation. *IEEE Trans.*
523 *Geosci. Remote Sens.* 52, 6315–6325.

524 Konings, A.G., Williams, A.P., Gentine, P., 2017. Sensitivity of grassland productivity to
525 aridity controlled by stomatal and xylem regulation. *Nat. Geosci.* 10, 284–288.
526 <https://doi.org/10.1038/ngeo2903>

527 Koster, R.D., Suarez, M.J., 2001. Soil moisture memory in climate models. *J.*
528 *Hydrometeorol.* 2, 558–570. [https://doi.org/10.1175/1525-](https://doi.org/10.1175/1525-7541(2001)002<0558:SMMICM>2.0.CO;2)
529 [7541\(2001\)002<0558:SMMICM>2.0.CO;2](https://doi.org/10.1175/1525-7541(2001)002<0558:SMMICM>2.0.CO;2)

530 Kramer, P.J., Boyer, J.S., 1995. *Water Relations of Plants and Soils*. Academic Press.

531 Kumar, S. V., Reichle, R.H., Koster, R.D., Crow, W.T., Peters-Lidard, C.D., 2009. Role
532 of subsurface physics in the assimilation of surface soil moisture observations. *J.*
533 *Hydrometeorol.* 10, 1534–1547. <https://doi.org/10.1175/2009JHM1134.1>

534 Kurum, M., Lang, R.H., O'Neill, P.E., Joseph, A.T., Jackson, T.J., Cosh, M.H., 2011. A
535 first-order radiative transfer model for microwave radiometry of forest canopies at L-
536 band. *IEEE Trans. Geosci. Remote Sens.* 49, 3167–3179.
537 <https://doi.org/10.1109/TGRS.2010.2091139>

538 Landsberg, J.J., Fowkes, N.D., 1978. Water Movement Through Plant Roots. *Ann. Bot.*
539 42, 493–508.

540 McColl, K.A., Alemohammad, S.H., Akbar, R., Konings, A.G., Yueh, S., Entekhabi, D.,
541 2017. The global distribution and dynamics of surface soil moisture. *Nat. Geosci.*
542 10, 100–104. <https://doi.org/10.1038/ngeo2868>

543 McCormick, E.L., Dralle, D.N., Hahm, W.J., Tune, A.K., Schmidt, L.M., Chadwick, K.D.,
544 Rempe, D.M., 2021. Widespread woody plant use of water stored in bedrock.
545 *Nature* 597, 225–229. <https://doi.org/10.1038/s41586-021-03761-3>

546 Miguez-Macho, G., Fan, Y., 2021. Spatiotemporal origin of soil water taken up by
547 vegetation. *Nature*.

548 Nadezhdina, N., David, T.S., David, J.S., Ferreira, M.I., Dohnal, M., Tesar, M., Gartner,
549 K., Leitgeb, E., Nadezhdin, V., Cermak, J., Jimenez, M.S., Morales, D., 2010. Trees
550 never rest: the multiple facets of hydraulic redistribution. *Ecohydrology* 3, 431–444.
551 <https://doi.org/10.1002/eco>

552 Nepstad, D.C., de Carvalho, C.R., Davidson, E.A., Jipp, P.H., Lefebvre, P.A., Negreiros,
553 G.H., da Silva, E.D., Stone, T.A., Trumbore, S.E., Vieira, S., 1994. The role of deep
554 roots in the hydrological and carbon cycles of Amazonian forests and pastures.
555 *Nature* 372, 666–669. <https://doi.org/10.1038/372666a0>

556 Nippert, J.B., Holdo, R.M., 2015. Challenging the maximum rooting depth paradigm in
557 grasslands and savannas. *Funct. Ecol.* 29, 739–745. <https://doi.org/10.1111/1365-2435.12390>

559 Nippert, J.B., Wieme, R.A., Ocheltree, T.W., Craine, J.M., 2012. Root characteristics of
560 C4 grasses limit reliance on deep soil water in tallgrass prairie. *Plant Soil* 355, 385–
561 394. <https://doi.org/10.1007/s11104-011-1112-4>

562 Njoku, E.G., Entekhabi, D., 1996. Passive microwave remote sensing of soil moisture.
563 *J. Hydrol.* 184, 101–129. [https://doi.org/10.1016/0022-1694\(95\)02970-2](https://doi.org/10.1016/0022-1694(95)02970-2)

564 Njoku, E.G., Kong, J.-A., 1977. Theory for passive microwave remote sensing of near-
565 surface soil moisture. *J. Geophys. Res.* 82, 3108.
566 <https://doi.org/10.1029/JB082i020p03108>

567 Ogle, K., Wolpert, R.L., Reynolds, J.F., 2004. Reconstructing plant root area and water
568 uptake profiles. *Ecology* 85, 1967–1978. <https://doi.org/10.1890/03-0346>

569 Paillou, P., Lopez, S., Farr, T., Rosenqvist, A., 2010. Mapping Subsurface Geology in
570 Sahara Using L-Band SAR: First Results From the ALOS/PALSAR Imaging Radar.
571 *IEEE J. Sel. Top. Appl. Earth Obs. Remote Sens.* 3, 632–636.
572 <https://doi.org/10.1109/JSTARS.2010.2056915>

573 Purdy, A.J., Fisher, J.B., Goulden, M.L., Colliander, A., Halverson, G., Tu, K.,
574 Famiglietti, J.S., 2018. SMAP soil moisture improves global evapotranspiration.
575 *Remote Sens. Environ.* 219, 1–14.
576 <https://doi.org/https://doi.org/10.1016/j.rse.2018.09.023>

577 Qiu, J., Crow, W.T., Nearing, G.S., 2016. The impact of vertical measurement depth on
578 the information content of soil moisture for latent heat flux estimation. *J.*
579 *Hydrometeorol.* 17, 2419–2430. <https://doi.org/10.1175/JHM-D-16-0044.1>

580 Qiu, J., Crow, W.T., Nearing, G.S., Mo, X., Liu, S., 2014. The impact of vertical
581 measurement depth on the information content of soil moisture times series data.
582 *Geophys. Res. Lett.* 41, 4997–5004.
583 <https://doi.org/10.1002/2014GL060017>.Received

584 Reichle, R.H., Liu, Q., Koster, R.D., Crow, W.T., 2019. Version 4 of the SMAP Level - 4
585 Soil Moisture Algorithm and Data Product. *J. Adv. Model. Earth Syst.* 11, 3106–

586 3130.

587 Rodell, M., Famiglietti, J.S., 2001. An analysis of terrestrial water storage variations in
588 Illinois with implications for the Gravity Recovery and Climate Experiment
589 (GRACE). *Water Resour. Res.* 37, 1327–1339.
590 <https://doi.org/10.1029/2000WR900306>

591 Santanello, J.A., Lawston, P., Kumar, S., Dennis, E., 2019. Understanding the impacts
592 of soil moisture initial conditions on NWP in the context of land-atmosphere
593 coupling. *J. Hydrometeorol.* 20, 793–819. <https://doi.org/10.1175/JHM-D-18-0186.1>

594 Schenk, H.J., Jackson, R.B., 2002. Rooting depths, lateral root spreads and below-
595 ground/above-ground allometries of plants in water-limited ecosystems. *J. Ecol.* 90,
596 480–494. <https://doi.org/10.1046/j.1365-2745.2002.00682.x>

597 Schenk, J.H., Jackson, R.B., 2002. the Global Biogeography of Roots. *Ecol. Monogr.*
598 72, 311–328. [https://doi.org/10.1890/0012-9615\(2002\)072\[0311:TGBOR\]2.0.CO;2](https://doi.org/10.1890/0012-9615(2002)072[0311:TGBOR]2.0.CO;2)

599 Schimel, D., Pavlick, R., Fisher, J.B., Asner, G.P., Saatchi, S., Townsend, P., Miller, C.,
600 Frankenberg, C., Hibbard, K., Cox, P., 2015. Observing terrestrial ecosystems and
601 the carbon cycle from space. *Glob. Chang. Biol.* 21, 1762–1776.
602 <https://doi.org/10.1111/gcb.12822>

603 Scott, R.L., Biederman, J.A., 2019. Critical Zone Water Balance Over 13 Years in a
604 Semiarid Savanna. *Water Resour. Res.* 55, 574–588.
605 <https://doi.org/10.1029/2018WR023477>

606 Short Gianotti, D.J., Akbar, R., Feldman, A.F., Salvucci, G.D., Entekhabi, D., 2020.
607 Terrestrial Evaporation and Moisture Drainage in a Warmer Climate. *Geophys.*
608 *Res. Lett.* 47, e2019GL086498. <https://doi.org/10.1029/2019GL086498>

609 Short Gianotti, D.J., Salvucci, G.D., Akbar, R., McColl, K.A., Cuenca, R., Entekhabi, D.,
610 2019. Landscape water storage and subsurface correlation from satellite surface
611 soil moisture and precipitation observations. *Water Resour. Res.* 9111–9132.
612 <https://doi.org/10.1029/2019wr025332>

613 Stocker, B.D., Tumber-d, S.J., Konings, A.G., Anderson, M.B., Hain, C., Jackson, R.B.,
614 2021. Global distribution of the rooting zone water storage capacity reflects plant
615 adaptation to the environment 1–20.

616 Taylor, C.M., De Jeu, R.A.M., Harris, P.P., Dorigo, W.A., Africa, W., 2012. Afternoon
617 rain more likely over drier soils. *Nature* 489, 423–426.
618 <https://doi.org/10.1038/nature11377>

619 Tumber-Dávila, S.J., Schenk, H.J., Du, E., Jackson, R.B., 2022. Plant sizes and shapes
620 above- and belowground and their interactions with climate. *New Phytol.*
621 <https://doi.org/10.1111/nph.18031>

622 Tuttle, S., Salvucci, G., 2016. Empirical evidence of contrasting soil moisture-
623 precipitation feedbacks across the United States. *Science* (80-). 352, 825–827.

624 Werner, C., Meredith, L.K., Ladd, S.N., Ingrisch, J., Kübert, A., van Haren, J., Bahn, M.,
625 Bailey, K., Bamberger, I., Beyer, M., Blomdahl, D., Byron, J., Daber, E., Deleeuw,
626 J., Dippold, M.A., Fudyma, J., Gil-Loaiza, J., Honeker, L.K., Hu, J., Huang, J.,
627 Klüpfel, T., Krechmer, J., Kreuzwieser, J., Kühnhammer, K., Lehmann, M.M.,
628 Meeran, K., Misztal, P.K., Ng, W.R., Pfannerstill, E., Pugliese, G., Purser, G.,
629 Roscioli, J., Shi, L., Tfaily, M., Williams, J., 2021. Ecosystem fluxes during drought
630 and recovery in an experimental forest. *Science* (80-). 374, 1514–1518.
631 <https://doi.org/10.1126/science.abj6789>

Table S1. Field isotropic tracer studies across the globe as displayed in Fig. 2. Crop species are specified and partitioned in the table due to wide variability of cultivated vegetation types (includes both herbaceous and woody species). Decay of water uptake with depth found in the study (1 = yes, 0 = no). Temporary plant uptake of upper layer soil moisture found in the study (1 = yes, 0 = no).

Reference	Reference Index	Plant Category	Latitude	Longitude	Mean Annual Precipitation (mm)	Uptake Range Top (cm)	Uptake Range Bottom (cm)	Isotope Sampling Months	Decay of Water Uptake With Depth	Temporary Uptake of Upper Layers
Meinzer et al. 1999	1	Tree	9	-79.5	2600	0	100	Jan. to May	0	1
Kulmatiski et al. 2010	2	Grass	-25	31.5	746	0	20	Oct., Nov., Feb., Apr.	1	0
Kulmatiski et al. 2010	2	Tree	-25	31.5	746	0	50	Oct., Nov., Feb., Apr.	0	0
Kulmatiski et al. 2013	3	Grass	-25	31.5	746	0	20	Nov., Feb., May	1	0
Kulmatiski et al. 2013	3	Tree	-25	31.5	746	0	20	Nov., Feb., May	1	0
Nippert and Knapp 2007	4	Grass	39	-96	850	0	30	Jun. to Aug.	1	0
Nippert and Knapp 2007	4	Shrub	39	-96	850	0	30	Jun. to Aug.	1	0
Le Roux et al. 1995	5	Grass	6.25	-5	1210	10	20	May, Nov., Jan.	0	0
Le Roux et al. 1995	5	Shrub	6.25	-5	1210	10	30	May, Nov., Jan.	0	0
Jackson et al. 1995	6	Tree	9	-79.5	2600	20	100	Dec. to May	0	0
Asbjornsen et al. 2008	7	Grass	41.5	-93	882	0	20	May to Sep.	0	0
Asbjornsen et al. 2008	7	Crop (Soybean)	41.5	-93	882	0	20	May to Sep.	0	0
Asbjornsen et al. 2008	7	Crop (Corn)	41.5	-93	882	0	20	May to Sep.	0	0
Asbjornsen et al. 2008	7	Shrub	41.5	-93	882	0	55	May to Sep.	1	1
Asbjornsen et al. 2008	7	Tree	41.5	-93	882	0	150	May to Sep.	0	1
Brooks et al. 2002	8	Tree	44	-121	550	0	200	Jul. to Sep.	0	1
Li et al. 2006	9	Tree	48	108.5	296	0	30	Jun. to Oct.	0	0
Schulze et al. 1996	10	Grass	-45.3	-69.8	125	0	30	Mar.	1	0
Schulze et al. 1996	10	Grass	-45.3	-70.3	160	0	30	Mar.	1	0
Schulze et al. 1996	10	Grass	-44.8	-71.3	290	0	30	Mar.	1	0
Schulze et al. 1996	10	Tree	-44.8	-71.6	770	0	80	Mar.	0	1
Ogle et al. 2004	11	Shrub	33	-107	230	0	70	Jul. to Aug.	1	1
Prechsl et al. 2015	12	Grass	47.2	8.3	1110	0	30	Apr. to Oct.	1	0
Prechsl et al. 2015	12	Grass	46.5	9.75	950	0	30	Apr. to Oct.	1	0

Eggemeyer et al. 2009	13	Grass	41.9	-100.3	573	5	50	Jan. to Nov.	0	0
Eggemeyer et al. 2009	13	Tree	41.9	-100.3	573	5	90	Jan. to Nov.	1	1
Hoekstra et al. 2014	14	Grass	47.47	8.9	927	0	40	Jun. to Aug.	0	0
Hoekstra et al. 2014	14	Grass	47.4	8.5	1176	0	40	Jun. to Aug.	0	0
Weltzin et al. 1997	15	Grass	31.5	-110.3	602	0	35	Apr., Sep.	1	0
Weltzin et al. 1997	15	Tree	31.5	-110.3	602	0	90	Apr., Sep.	0	1
Moreira et al. 2000	16	Grass	-3	-47	1800	0	100	Apr. Jun., Jul., Dec.	1	0
Moreira et al. 2000	16	Shrub	-3	-47	1800	0	25	Apr. Jun., Jul., Dec.	0	0
Retzlaff et al. 2001	17	Tree	34.8	-79.6	1200	0	120	Mar. to Nov.	1	1
Jackson et al. 1999	18	Tree	-15.8	-47.8	1550	0	300	Aug., Sep.	0	0
Plamboeck et al. 1999	19	Tree	64.25	19.75	614	0	55	Jul., Aug.	1	0
Wu et al. 2014	20	Shrub	44.25	87.75	160	0	300	Mar. to Oct.	0	0
Wu et al. 2014	20	Shrub	44.25	87.75	160	0	60	Mar. to Oct.	1	0
Ohte et al. 2003	21	Tree	39	109.15	362	0	150	Sep.	0	0
Ohte et al. 2003	21	Shrub	39	109.15	362	0	50	Sep.	1	0
Goldsmith et al. 2012	22	Tree	19.75	-97	3186	0	40	Mar., May	0	0
Goldsmith et al. 2012	22	Tree	19.75	-97	3186	60	80	Mar., May	0	0
Hartsough et al. 2008	23	Tree	19.5	-103.5	1100	0	30	Mar., Nov.	0	0
Liu et al. 2010	24	Tree	21.9	101.25	1487	0	60	Mar., Dec.	0	1
Liu et al. 2010	24	Tree	21.9	101.25	1487	0	150	Mar., Dec.	0	1
Chimner et al. 2004	25	Shrub	37.7	-105.8	121	0	200	Jun., Aug.	0	1
Williams et al. 2000	26	Tree	34	-110	430	0	50	May to Sep.	0	1
Williams et al. 2000	26	Tree	39	-110	390	0	50	May to Sep.	0	1
Williams et al. 2000	26	Tree	39	-110	390	50	100	May to Sep.	0	0
Dai et al. 2015	27	Shrub	44.33	87.9	125	0	300	Apr. to Sep.	0	1
Yang et al. 2015	28	Crop (Corn)	38.5	100.33	129	0	10	Apr. to Sep.	0	0
Zhu et al. 2011	29	Shrub	38.5	103	111	0	120	May, Jul., Sep.	0	1
Ma et al. 2018	30	Crop (Wheat)	39.5	116.5	540	0	70	Jul., Aug.	1	1
Munoz-Villers et al. 2020	31	Crop (Coffee)	19.5	-97	1765	0	15	Jan. to May, Aug.	0	0
Munoz-Villers et al. 2020	31	Tree	19.5	-97	1765	0	120	Jan. to May, Aug.	1	1
Ellsworth et al. 2015	32	Tree	27.2	-81.33	1346	20	150	Jan. to Dec.	0	0
Wu et al. 2016	33	Crop (Corn)	37.8	102.9	164	0	80	Jun. to Aug.	1	1
Liu et al. 2019	34	Tree	37.5	114.5	521	0	40	Mar. to Sep.	0	0
Asbjornsen et al. 2007	35	Crop (Corn)	41.5	-93.25	882	0	20	Jul.	0	0

Wang et al. 2010	36	Crop (Corn)	34.9	110.75	590	0	50	May to Oct.	1	1
Wang et al. 2010	36	Crop (Cotton)	34.9	110.75	590	0	90	May to Oct.	1	1
Liu et al. 2011	37	Shrub	30.85	103	711	0	30	Aug.	0	0
Ratajczak et al. 2011	38	Shrub	39.1	-96.6	835	0	75	Jun. to Sep.	1	0
Ratajczak et al. 2011	38	Grass	39.1	-96.6	835	0	30	Jun. to Sep.	1	0
Case et al. 2020	39	Grass	-24	31.5	479	0	10	May, Jun.	0	0
Case et al. 2020	39	Tree	-24	31.5	479	0	50	May, Jun.	1	1
Case et al. 2020	39	Grass	-24	31.5	510	0	20	May, Jun.	1	0
Case et al. 2020	39	Tree	-24	31.5	510	0	100	May, Jun.	0	0
Case et al. 2020	39	Grass	-24	31.5	600	0	50	May, Jun.	1	1
Case et al. 2020	39	Tree	-24	31.5	600	0	100	May, Jun.	1	1
Hahn et al. 2021	40	Tree	0.5	35.3	1988	0	150	Sep. to Dec.	1	1
Brinkmann et al. 2019	41	Tree	47.5	8.3	1110	0	70	Apr. to Nov.	0	1
Sun et al. 2021	42	Crop (Pea)	47.5	8.5	994	0	20	May to Jul.	1	0
Sun et al. 2021	42	Crop (Barley)	47.5	8.5	994	0	60	May to Jul.	1	0
Clement et al. 2022	43	Crop (Alfalfa)	55.7	12.3	523	0	100	Jun. to Aug.	1	1
Clement et al. 2022	43	Crop (Wheatgrass)	55.7	12.3	523	0	100	Jun. to Aug.	1	1
Bachmann et al. 2015	44	Grass	50.9	11.5	587	0	10	Apr., Jun., Sep.	0	0
Penna et al. 2021	45	Crop (Apple Tree)	46.6	10.7	480	0	40	Jun. to Sep.	1	0

References

1. Meinzer, F. C. *et al.* Partitioning of soil water among canopy trees in a seasonally dry tropical forest. *Oecologia* 293–301 (1999). doi:10.1007/s004420050931
2. Kulmatiski, A., Beard, K. H., Verweij, R. J. T. & February, E. C. A depth-controlled tracer technique measures vertical, horizontal and temporal patterns of water use by trees and grasses in a subtropical savanna. *New Phytol.* **188**, 199–209 (2010).
3. Kulmatiski, A. & Beard, K. H. Root niche partitioning among grasses, saplings, and trees measured using a tracer technique. *Oecologia* **171**, 25–37 (2013).
4. Nippert, J. B. & Knapp, A. K. Linking water uptake with rooting patterns in grassland species. *Oecologia* **153**, 261–272 (2007).
5. Le Roux, X., Bariac, T. & Mariotti, A. Spatial Partitioning of the Soil Water Resource between Grass and Shrub Components in a West African Humid Savanna. *Oecologia* **104**, 147–155 (1995).
6. Jackson, P. C., Cavelier, J., Goldstein, G., Meinzer, F. C. & Holbrook, N. M.

- Partitioning of water resources among plants of a lowland tropical forest. *Oecologia* **101**, 197–203 (1995).
7. Asbjornsen, H., Shepherd, G., Helmers, M. & Mora, G. Seasonal patterns in depth of water uptake under contrasting annual and perennial systems in the Corn Belt Region of the Midwestern U.S. *Plant Soil* **308**, 69–92 (2008).
 8. Brooks, J. R., Meinzer, F. C., Coulombe, R. & Gregg, J. Hydraulic redistribution of soil water during summer drought in two contrasting Pacific Northwest coniferous forests. *Tree Physiol.* **22**, 1107–1117 (2002).
 9. Li, S. G. *et al.* Seasonal variation in oxygen isotope composition of waters for a montane larch forest in Mongolia. *Trees - Struct. Funct.* **20**, 122–130 (2006).
 10. Schulze, E. D. *et al.* Rooting depth, water availability, and vegetation cover along an aridity gradient in Patagonia. *Oecologia* **108**, 503–511 (1996).
 11. Ogle, K., Wolpert, R. L. & Reynolds, J. F. Reconstructing plant root area and water uptake profiles. *Ecology* **85**, 1967–1978 (2004).
 12. Prechsl, U. E., Burri, S., Gilgen, A. K., Kahmen, A. & Buchmann, N. No shift to a deeper water uptake depth in response to summer drought of two lowland and sub-alpine C3-grasslands in Switzerland. *Oecologia* **177**, 97–111 (2015).
 13. Eggemeyer, K. D. *et al.* Seasonal changes in depth of water uptake for encroaching trees *Juniperus virginiana* and *Pinus ponderosa* and two dominant C4 grasses in a semiarid grassland. *Tree Physiol.* **29**, 157–169 (2009).
 14. Hoekstra, N. J., Finn, J. A., Hofer, D. & Lüscher, A. The effect of drought and interspecific interactions on depth of water uptake in deep- and shallow-rooting grassland species as determined by $\delta^{18}\text{O}$ natural abundance. *Biogeosciences* **11**, 4493–4506 (2014).
 15. Weltzin, J. F. & McPherson, G. R. Spatial and temporal soil moisture resource partitioning by trees and grasses in a temperate savanna, Arizona, USA. *Oecologia* **112**, 156–164 (1997).
 16. Moreira, M. Z., Sternberg, L. da S. L. & Nepstad, D. C. Vertical patterns of soil water uptake by plants in a primary forest and an abandoned pasture in the eastern Amazon: An isotopic approach. *Plant Soil* **222**, 95–107 (2000).
 17. Retzlaff, W. A., Blaisdell, G. K. & Topa, M. A. Seasonal changes in water source of four families of loblolly pine (*Pinus taeda* L.). *Trees - Struct. Funct.* **15**, 154–162 (2001).
 18. Jackson, P. C. *et al.* Partitioning of soil water among tree species in a Brazilian Cerrado ecosystem. *Tree Physiol.* **19**, 717–724 (1999).
 19. Plamboeck, A. H., Grip, H. & Nygren, U. A hydrological tracer study of water uptake depth in a Scots pine forest under two different water regimes. *Oecologia* **119**, 452–460 (1999).
 20. Wu, Y., Zhou, H., Zheng, X. J., Li, Y. & Tang, L. S. Seasonal changes in the water use strategies of three co-occurring desert shrubs. *Hydrol. Process.* **28**, 6265–6275 (2014).
 21. Ohte, N. *et al.* Water Utilization of Natural and Planted Trees in the Semiarid Desert of Inner Mongolia, China. Published by: Ecological Society of America WATER UTILIZATION OF NATURAL AND PLANTED TREES IN THE SEMIARID DESERT OF INNER MONGOLIA, CHINA. *Ecol. Appl.* **13**, 337–351 (2003).
 22. Goldsmith, G. R. *et al.* Stable isotopes reveal linkages among ecohydrological

- processes in a seasonally dry tropical montane cloud forest. *Ecohydrology* **5**, 779–790 (2012).
23. Hartsough, P., Poulson, S. R., Biondi, F. & Estrada, I. G. Stable isotope characterization of the ecohydrological cycle at a tropical treeline site. *Arctic, Antarct. Alp. Res.* **40**, 343–354 (2008).
 24. Liu, W., Liu, W., Li, P., Duan, W. & Li, H. Dry season water uptake by two dominant canopy tree species in a tropical seasonal rainforest of Xishuangbanna, SW China. *Agric. For. Meteorol.* **150**, 380–388 (2010).
 25. Chimner, R. A. & Cooper, D. J. Using stable oxygen isotopes to quantify the water source used for transpiration by native shrubs in the San Luis Valley, Colorado U.S.A. *Plant Soil* **260**, 225–236 (2004).
 26. Williams, D. G. & Ehleringer, J. R. Intra- and interspecific variation for summer precipitation use in pinyon-juniper woodlands. *Ecol. Monogr.* **70**, 517–537 (2000).
 27. Dai, Y., Zheng, X.-J., Tang, L.-S. & Li, Y. Stable oxygen isotopes reveal distinct water use patterns of two *Haloxylon* species in the Gurbantonggut Desert. *Plant Soil* **389**, 73–87 (2015).
 28. Yang, B., Wen, X. & Sun, X. Irrigation depth far exceeds water uptake depth in an oasis cropland in the middle reaches of Heihe River Basin. *Sci. Rep.* **5**, 1–12 (2015).
 29. Zhu, Y., Jia, Z. & Yang, X. Resource-dependent water use strategy of two desert shrubs on interdune, Northwest China. *J. Food, Agric. Environ.* **9**, 832–835 (2011).
 30. Ma, Y. & Song, X. Seasonal variations in water uptake patterns of winter wheat under different irrigation and fertilization treatments. *Water (Switzerland)* **10**, (2018).
 31. Muñoz-Villers, L. E., Geris, J., Alvarado-Barrientos, M. S., Holwerda, F. & Dawson, T. Coffee and shade trees show complementary use of soil water in a traditional agroforestry ecosystem. *Hydrol. Earth Syst. Sci.* **24**, 1649–1668 (2020).
 32. Ellsworth, P. Z. & Sternberg, L. S. L. Seasonal water use by deciduous and evergreen woody species in a scrub community is based on water availability and root distribution. *Ecohydrology* **8**, 538–551 (2015).
 33. Wu, Y. *et al.* Quantification of maize water uptake from different layers and root zones under alternate furrow irrigation using stable oxygen isotope. *Agric. Water Manag.* **168**, 35–44 (2016).
 34. Liu, Y. *et al.* The depth of water taken up by Walnut trees during different phenological stages in an irrigated arid hilly area in the Taihang Mountains. *Forests* **10**, (2019).
 35. Asbjornsen, H., Mora, G. & Helmers, M. J. Variation in water uptake dynamics among contrasting agricultural and native plant communities in the Midwestern U.S. *Agric. Ecosyst. Environ.* **121**, 343–356 (2007).
 36. Wang, P., Song, X., Han, D., Zhang, Y. & Liu, X. A study of root water uptake of crops indicated by hydrogen and oxygen stable isotope: A case in Shanxi Province, China. *Agric. Water Manag.* **97**, 475–482 (2010).
 37. Liu, Y. *et al.* Analyzing relationships among water uptake patterns, rootlet biomass distribution and soil water content profile in a subalpine shrubland using water isotopes. *Eur. J. Soil Biol.* **47**, 380–386 (2011).

38. Ratajczak, Z., Nippert, J. B., Hartman, J. C. & Ocheltree, T. W. Positive feedbacks amplify rates of woody encroachment in mesic tallgrass prairie. *Ecosphere* **2**, (2011).
39. Case, M. F., Nippert, J. B., Holdo, R. M. & Staver, A. C. Root-niche separation between savanna trees and grasses is greater on sandier soils. *J. Ecol.* **108**, 2298–2308 (2020).
40. Hahn, M., Jacobs, S. R., Breuer, L., Rufino, M. C. & Windhorst, D. Variability in tree water uptake determined with stable water isotopes in an African tropical montane forest. *Ecohydrology* **14**, 1–14 (2021).
41. Brinkmann, N., Eugster, W., Buchmann, N. & Kahmen, A. Species-specific differences in water uptake depth of mature temperate trees vary with water availability in the soil. *Plant Biol.* **21**, 71–81 (2019).
42. Sun, Q. *et al.* Water uptake patterns of pea and barley responded to drought but not to cropping systems. *Biogeosciences Discuss.* 1–37 (2021). doi:10.5194/bg-2021-217
43. Clément, C. *et al.* Comparing the deep root growth and water uptake of intermediate wheatgrass (Kernza®) to alfalfa. *Plant Soil* **472**, 369–390 (2022).
44. Bachmann, D. *et al.* No evidence of complementary water use along a plant species richness gradient in temperate experimental grasslands. *PLoS One* **10**, 1–14 (2015).
45. Penna, D. *et al.* Water uptake of apple trees in the Alps: Where does irrigation water go? *Ecohydrology* **14**, 1–16 (2021).

